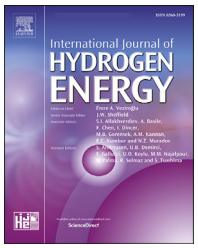
Available online at www.sciencedirect.com

ScienceDirect

journal homepage: www.elsevier.com/locate/he



Low temperature catalytic activity of hydrothermally synthesised ruthenium promoted ceria-zirconia composites for reforming CO_2-rich methane

Jason Sun [a,b], *Doki Yamaguchi* [b,**], *Liangguang Tang* [b], *Anita M. D'Angelo* [c], *Ken Chiang* [a,*]

[a] *School of Engineering, RMIT University, Melbourne, VIC 3000, Australia*
[b] *CSIRO Energy, Private Bag 10, Clayton South, VIC 3168, Australia*
[c] *Australian Synchrotron (ANSTO), Clayton, VIC 3168, Australia*

HIGHLIGHTS

- A trace amount of Ru (0.10 wt%) was used to promote ceria-zirconia.
- 0.10 wt% Ru significantly increased its reducibility and oxygen exchange dynamics.
- Synthesis method showed a performance difference at temperatures between 400 and 850 °C.
- 44% of CH_4 and 57.4% CO_2 were converted at 600 °C by 0.1Ru1CZ5U-180.
- No observable carbon formation was detected from hydrothermally prepared samples.

ARTICLE INFO

Article history:
Received 22 February 2023
Received in revised form
8 May 2023
Accepted 8 July 2023
Available online 25 July 2023

Keywords:
Ruthenium
Ceria
Zirconia
Dry reforming of methane
Syngas
Low temperature

ABSTRACT

The use of CO_2-rich natural gas as feedstock in DRM is an attractive route of carbon dioxide utilisation due to the compositional advantage of these particular resources. The optimal operating conditions would potentially improve the overall thermal efficiency of the DRM process, especially when the temperature is lower than 800 °C. This study reports a catalyst with the demonstrated high performance and high coke-resistance, developed from ruthenium modified ceria-zirconia. Coprecipitation and hydrothermal methods were adopted to prepare the ceria-zirconia supports, and then impregnated with a very small amount of Ru (0.10 wt%). The structure-catalytic activity relationship of the catalyst was further investigated in DRM. High conversions of CH_4 and CO_2, i.e., 44.0% and 57.4%, respectively, were achieved by using 0.1Ru1CZ5U-180 at low temperature of 600 °C. A significant reduction in the onset reaction temperature was observed from temperature programmed reduction (TPR) and this observation was related to the increased number of exchangeable oxygens in the presence of Ru. Nitrogen adsorption-desorption results suggested that the specific surface area and the total pore volume also improved the exchange of oxygen between adsorbed carbon dioxide molecules and the crystal lattice. It is evident that the presence of ruthenium accelerated the oxygen spillover process on the surface of the catalyst, and facilitated the dynamics of the oxygen exchange between the adsorbed carbon dioxide molecules and the ceria-zirconia, which ultimately contributed to the

* *Corresponding author.*
** *Corresponding author.*
E-mail addresses: Doki.Yamaguchi@csiro.au (D. Yamaguchi), Ken.Chiang@rmit.edu.au (K. Chiang).
https://doi.org/10.1016/j.ijhydene.2023.07.079
0360-3199/Crown Copyright © 2023 Published by Elsevier Ltd on behalf of Hydrogen Energy Publications LLC. This is an open access article under the CC BY-NC-ND license (http://creativecommons.org/licenses/by-nc-nd/4.0/).

observed increase in catalytic activity at temperatures below 800 °C. Most importantly, no detectable carbon deposits were formed over the entire experimental period when the ruthenium modified ceria-zirconia catalyst was used.

Crown Copyright © 2023 Published by Elsevier Ltd on behalf of Hydrogen Energy Publications LLC. This is an open access article under the CC BY-NC-ND license (http://creativecommons.org/licenses/by-nc-nd/4.0/).

Introduction

Due to the continued issue of climate change, the strong push to transition to renewable or clean energy is more urgent than ever. One of the effective solutions is to reduce the carbon emission by developing carbon capture, utilisation, and storage technologies. Dry reforming of methane (DRM) is deemed to be a promising pathway where two greenhouse gases CH_4 and CO_2 are equimolarly converted into synthesis gas, i.e., a mixture of hydrogen and carbon monoxide. Synthesis gas or simply syngas has been widely used as a precursor for manufacturing chemicals including ammonia (53%), H_2 (23%), and methanol (11%) [1,2]. It can also be used to produce synthetic liquid fuels via established technologies such as Fischer–Tropsch process and dimethyl ether synthesis.

Recently, there is an increased interest in developing low-temperature DRM process, owing to the potential advantages of: 1) the increased thermal efficiency, 2) the reduced operating cost, and 3) the enhanced process integration and intensification (e.g., the production of fuel-cell grade hydrogen by coupling reforming processes and membrane separation) [3–10]. However, carbon formation is favoured in the temperature range of 557–700 °C due to the preferential occurrence of methane cracking and/or Boudouard reaction [11], the successful implementation of low-temperature DRM (<700 °C) would be enticing.

The oxide supports are pivotal in the achieving low-temperature catalytic performance of DRM. The oxide supports, such as silica, alumina, mixed oxides (e.g., CeO_2–ZrO_2, Al_2O_3–MgO), and perovskites [12–14], not only serve as essential components in DRM catalysts, but also provide an added functionality of storing and releasing oxygen. This property allows a dynamic exchange of oxygen atoms between the solid catalysts with the surrounding atmosphere. These stoichiometric changes in oxygen from the oxide materials are indeed a key contributor to the catalytic functioning of oxide materials [15,16]. As such, ceria (CeO_2) was used in this work to utilise the excellent oxygen storage capacity (OSC) derived from its facile and cyclic redox between Ce^{4+} and Ce^{3+} in the oxide.

Recent discoveries have shown that the formation of the preferential exposed ceria facets from different synthesis approaches could promote the catalytic activity and product selectivity in the hydrogenation and reforming reactions [17]. It was also demonstrated that low index ceria facets (100) were more effective in enhancing the catalytic activities, for example, CO_2 methanation [18] and reverse water gas shift reaction (RWGS) [19]. The addition of zirconia into ceria (smaller ionic radius, i.e., Zr^{4+} 0.84 Å < Ce^{4+} 0.97 Å) induced more structural defects due to its effect on the increase of the lattice strain, giving rise to the content of oxygen vacancies in ceria-zirconia (CZ) composites. The presence of oxygen vacancies can significantly alter the degree of oxygen mobility, contributing their lattice oxygen in many catalytic systems. The formation of oxygen vacancies can be described as Kröger-Vink notation:

$$O_O^x + 2\,Ce_{Ce}^x \rightarrow V_O^{\cdot\cdot} + 2\,Ce_{Ce}' + 0.5\,O_2 \quad (1)$$

where O_O^x and $V_O^{\cdot\cdot}$ represent lattice oxygen and oxygen vacancy in the normal lattice oxygen position, respectively, while Ce_{Ce}^x and Ce_{Ce}' represent Ce^{3+} and Ce^{4+}, respectively, in the crystal lattice. The fluorite structure of ceria remained unchanged despite the occurrence of severe oxygen defects in the crystal lattice. Violi et al. [20] and Dong et al. [21] both highlighted the important role of structural defects played in improving OSC and the oxygen mobility in CZ composites. Balducci et al. [22] also revealed the contribution of that ceria lattice decrease in CZ composites in decreasing the Ce^{4+}/Ce^{3+} reduction energy on the stable (110) and (111) surfaces, further facilitating lowering its bulk reduction energy.

Apart from the addition of Zr, the introduction of trace amounts of platinum group metals (PGMs) was also found to effectively alter the diffusion rate of lattice oxygen as well as the reversible spill-over of oxygen between the metallic particles and CZ supports. The effective exchange of lattice oxygen at the metal-support interface promoted the catalytic activity in accordance with the Mars-van Krevelen (MvK) mechanism. Our recent work showed that the modification of CZ samples with metallic ruthenium (Ru) enhanced the oxygen exchanging capability and increased the reducibility at lower temperatures [16]. On top of that, coke resistance was also dramatically improved by adding a small amount of Ru in our work and [23,24]. All studies showed that the small loading amount of Ru is sufficient and effective in improving DRM performance. However, excessive amount of Ru (>1.5 wt%) can cause a dramatic decrease in surface areas and pore volumes, which in turn lowered the OSC and the degree of oxygen mobility of ceria [25]. Therefore, a small loading amount of Ru could be sufficient to produce promising catalytic conversions at low temperature (<700 °C).

Despite the fact that there is a large body of literature regarding the preparation of CZ materials, such as coprecipitation (CP) [26], sol-gel [27], high energy ball-milling [28], flame-spray pyrolysis [29], co-impregnation [30], and hydrothermal method [31], hydrothermal method is one of the most promising synthesis approaches to prepare and control the morphologies of CZ materials due to the mild synthesis conditions [32,33]. A few research works have been devoted to studying ceria mixed oxides in different shapes [34,35]. A challenge remains in controlling the morphologies of CZ materials and establishing the critical structure-catalytic activity relationships in most studies. This work therefore aims to

evaluate (i) the structural and morphological properties of CZ prepared by hydrothermal method, and (ii) the catalytic performance of CZ samples and Ru impregnated CZ samples (as low as 0.10 wt%) for DRM at low temperatures (<700 °C). The effects of several process parameters including reaction time and temperature, on the formation of morphologies and catalytic performance will be reported. The effect of Ru on the carbon formation will also be discussed.

Experimental section

Catalyst preparation

All analytical grade chemicals were used without further treatment in this study. Ceria-zirconia (CZ) samples were synthesised by the hydrothermal method as described in the next section and the coprecipitation method for benchmarking purpose [16]. Ruthenium was impregnated to CZ samples by the wet impregnation method.

Hydrothermal synthesis

CZ samples were hydrothermally prepared in a fixed 3: 1 M ratio of ceria to zirconia. The molar ratio was determined to be optimum in an earlier study and therefore was adopted without modification. Pre-determined amounts of cerium (III) nitrate hexahydrate [$Ce(NO_3)_3 \cdot 6H_2O$, Aldrich], zirconyl (IV) nitrate hydrate [$ZrO(NO_3)_2 \cdot xH_2O$, Aldrich], and urea [$CO(NH_2)_2$, Chem-Supply] were dissolved in deionised water to form a final mixture with 0.03 M of cerium (III) nitrate hexahydrate and 0.01 M of zirconyl (IV) nitrate hydrate.

The effect of urea concentration on the properties of the resulting CZ samples was studied by varying the amount of urea added to the hydrothermal reaction. The final concentration of urea was fixed to either two or five times of the stoichiometric requirement (CZ/U) for the complete hydrolysis of both cerium and zirconium ions. After mixing the precursors together, the resulting mixture was transferred to a 100 mL Teflon®-lined autoclave for hydrothermal treatment.

To investigate the effect of the hydrothermal temperatures on the morphologies of CZ samples, two different temperatures were chosen in this study, i.e., 120 °C and 180 °C. In a typical run, the hydrothermal reaction was kept at the designated temperature for 6 h. Then the sample contained in the autoclave was cooled to room temperature naturally. The resulting precipitates were collected by filtration, washed repeatedly with deionised water, and dried in an oven at 80 °C overnight. All the dried samples were calcined in a tube furnace at 650 °C for 4 h at a constant heating rate of 5 °C/min under a steady flow of air. The as-prepared CZ samples under different hydrothermal conditions were denoted as 1CZ2U-120, 1CZ2U-180, 1CZ5U-120 and 1CZ5U-180, respectively.

Coprecipitation method

For the purpose of benchmarking, CZ samples were also prepared by coprecipitation with the use of urea as the precipitating agent in our previous work [16]. The as-prepared CZ sample was denoted as Ce75Zr25.

Wetness impregnation

Once ceria-zirconia samples were obtained from either the hydrothermal method or coprecipitation method, they were impregnated with ruthenium via the wetness impregnation. In this method, Ru (III) acetylacetonate [$(C_5H_7O_2)_3Ru$, Aldrich] was used as the ruthenium precursor. The nominal ruthenium (Ru) loading of 0.10 wt% was fixed in this study. After impregnation, all the samples were dried in an oven at 80 °C overnight, and then calcined at 650 °C for 4 h under a constant flow of air. The resulting catalysts were denoted as 0.1RuCe75Zr25, 0.1Ru1CZ2U-120, 0.1Ru1CZ2U-180, 0.1Ru1CZ5U-120 and 0.1Ru1CZ5U-180, separately. A collection of samples used in this study is summarised in Table 1.

Materials characterisation

X-ray diffraction (XRD)

The crystallinity of samples was examined by using a Bruker Axs D4 Endeavour Wide angle diffractometer with Cu Kα radiation (40 kV, 200 mA) and a Ni filter ($\lambda = 0.15406$ nm) at a scanning rate of 0.02°/s, in the 2θ range of 10°–90°. The calculations of lattice parameter and the average crystallite size were determined by using the same method described in the previous work [16].

Specific surface area measurements

The N_2 adsorption - desorption measurements of the samples were performed in Micromeritics Tristar based at −196 °C. The data obtained from the adsorption isotherm were then correlated to their specific surface area by mean of the Brunauer–Emmett–Teller (BET) correlation. All the samples were degassed at 250 °C overnight before commencing the measurement. The total pore volume and the average pore size were acquired from the maximum adsorption point at $P/P_0 = 0.99$ and the Barrett-Joyner-Halenda (BJH) equation from the desorption isotherm, respectively.

Scanning electron microscope (SEM)

FEI Quanta 200 SEM was used to investigate the morphologies of all samples. The operating acceleration voltage was 15–30 kV with the magnification values varying between 100 and 10000. Prior to analysis, all samples were sputtered on a

Table 1 – A summary of samples discussed in this study.

Base sample preparation method	Samples	Ru loading wt%	CZ/U ratio –	Reaction temperature °C
Coprecipitation	Ce75Zr25	0	1	100
Hydrothermal method	1CZ2U-120	0	1/2	120
	1CZ2U-180	0	1/2	180
	1CZ5U-120	0	1/5	120
	1CZ5U-180	0	1/5	180
Wet impregnation	0.1RuCe75Zr25	0.1	1	100
	0.1Ru1CZ2U-120	0.1	1/2	120
	0.1Ru1CZ2U-180	0.1	1/2	180
	0.1Ru1CZ5U-120	0.1	1/5	120
	0.1Ru1CZ5U-180	0.1	1/5	180

conductive carbon tape and coated with a 3 nm thickness of iridium.

Temperature-programmed reduction (TPR)

The reduction profiles of CZ samples and Ru-impregnated CZ samples were studied by TPR analyses, performed in a thermogravimetric analyser (TGA, PerkinElmer Pyris 1 TGA). A typical sample run was conducted with a drying step at 150 °C under Ar for 1 h and then cooled to 50 °C. The sample was subsequently heated in a flow of 4 vol% H_2/Ar at a constant ramping rate of 5 °C/min from 50 °C to 900 °C. The weight loss was ascribed to the reduction of the samples due to the oxygen removal from the sample by H_2. The oxygen storage capacity (OSC) was quantified from the amount of oxygen removal on the basis of per unit of mass of the sample at a particular cut-off temperature of interest. The differential weight loss curve derived from the Derivative Thermogravimetry (DTG) was used to evaluate the reduction properties of all the samples.

Temperature programmed oxidation (TPO)

The amount of carbon deposited on the used samples was calculated from the mass balance of carbon by considering the amounts of CH_4, CO_2, CO, and complemented by the post-reaction TGA carbon burn-off analyses to account for any solid carbon formed on the surface of catalysts. A typical TGA run was performed by heating the sample in a flow of air from room temperature to 800 °C at a constant ramping rate of 5 °C/min. Any weight loss would be considered as the oxidation of the carbon deposits on the solid surface, corresponding to the carbon closure as percentage.

Catalyst activity testing

The catalytic activity of all the samples for DRM was studied in a continuous flow fixed-bed reactor at atmospheric pressure. Typically, 1.0 g of the sample was loaded and positioned in the centre of a quartz tube (12 mm OD, 8 mm ID and 390 mm length). A K-type thermocouple was used to monitor the bed temperature during the reaction. A gas premix containing a 1:1 volumetric ratio of CH_4 to CO_2 was introduced into the reactor. The gas premix also contained 5 vol% of Ar that was used as an internal standard for quantification purpose. DRM reaction was taken place at a constant volumetric rate of 50 mL/min. Under such conditions, the weight hourly space velocity was 3000 L/(h·kg-cat). The effluent gases leaving the reactor were cooled in a cold trap and then analysed by an online gas chromatograph (GC, PerkinElmer 580) equipped with a thermal conductivity detector (TCD). In this study, the activity of each sample was evaluated isothermally at temperatures between 400 °C and 850 °C. The steady-state conversions of CH_4 (X_{CH_4}) and CO_2 (X_{CO_2}) at each temperature were determined based on the molar concentrations of the gases in the inlet and the outlet of the reactor. Different quantities that were used to assess the catalyst performance are expressed in Eqs. (2)–(6):

$$\text{CH}_4\text{ conversion [\%]} : X_{CH_4} = \left(F_{CH_{4,in}} - F_{CH_{4,out}}\right) \Big/ F_{CH_{4,in}} \times 100 \quad (2)$$

$$\text{CO}_2\text{ conversion [\%]} : X_{CO_2} = \left(F_{CO_{2,in}} - F_{CO_{2,out}}\right) \Big/ F_{CO_{2,in}} \times 100 \quad (3)$$

$$\text{H}_2/\text{CO ratio} : H_2/CO = Y_{H_2}/Y_{CO} \quad (4)$$

$$\text{H}_2\text{ yield} : Y_{H_2} = F_{H_{2,out}} \Big/ \left[2\left(F_{CH_{4,in}} - F_{CH_{4,out}}\right)\right] \times 100\% \quad (5)$$

$$\text{CO yield} : Y_{CO} = F_{CO_{out}} \Big/ \left[\left(F_{CH_{4,in}} - F_{CH_{4,out}}\right) + \left(F_{CO_{2,in}} - F_{CO_{2,out}}\right)\right] \times 100\% \quad (6)$$

where $F_{CH_{4,in}}$ and $F_{CO_{2,in}}$ are the molar flow rates of CH_4 and CO_2 in the inlet of the reactor, respectively, and $F_{CH_{4,out}}$, $F_{CO_{2,out}}$, $F_{H_{2,out}}$, and $F_{CO_{out}}$ are the molar flow rates of CH_4, CO_2, H_2, and CO at the outlet of the reactor, respectively.

Results and discussion

Textural and structural properties

Table 2 summaries the textural properties of CZ and Ru-impregnated CZ samples, including their specific surface

Table 2 – Textural and structural properties of CZ samples and 0.1Ru-impregnated CZ samples.

Sample	Specific surface areas	Total pore volumes	Mean pore sizes	Crystallite sizes	Lattice parameters
	m^2/g	cm^3/g	nm	nm	nm
Ce75Zr25	26	0.07	86	13.0	0.540
1CZ2U-120	41	0.06	5.5	17.3	0.540
1CZ2U-180	50	0.14	10.3	14.2	0.540
1CZ5U-120	69	0.21	10.1	8.8	0.541
1CZ5U-180	71	0.32	14.9	8.8	0.539
0.1RuCe75Zr25	18	0.06	98	21.5	0.541
0.1Ru1CZ2U-120	41	0.06	5.3	17.5	0.540
0.1Ru1CZ2U-180	51	0.14	9.5	14.4	0.540
0.1Ru1CZ5U-120	60	0.20	11.0	9.4	0.540
0.1Ru1CZ5U-180	71	0.33	15.5	9.0	0.539

[a] calculated by using the BET correlation.
[b] estimated from the maximum adsorption point at $P/P_0 = 0.99$.
[c] determined from BJH desorption isotherm for average pore diameter.
[d] calculated from the X-ray diffraction of CeO_2 (111) plane using Scherrer equation.

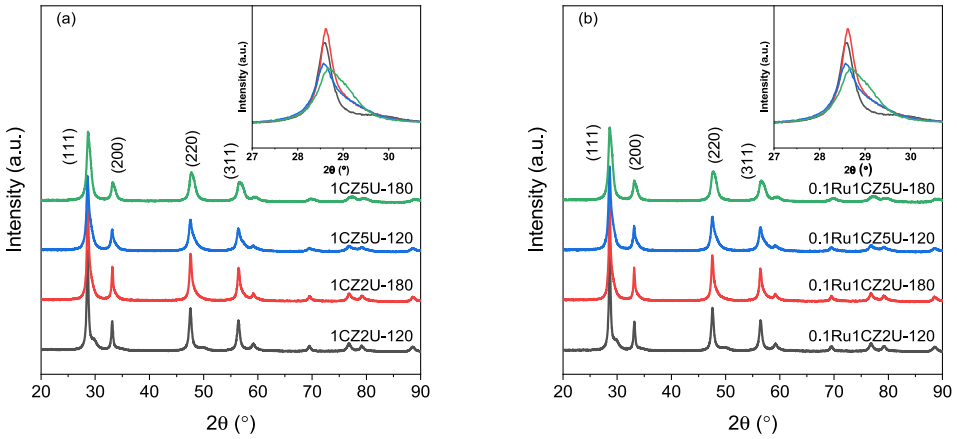


Fig. 1 – XRD patterns of (a) CZ and (b) Ru-impregnated CZ samples.

areas (SSAs), total pore volumes, mean pore sizes, crystallite sizes and lattice parameters. The SSA measurement clearly showed that the synthesis methods had a significant effect on the SSAs of samples. Hydrothermally prepared CZ samples presented approximately twice larger SSAs than that of coprecipitated CZ samples. Another important finding with the hydrothermal method was that either the use of higher hydrothermal reaction temperature or an excess amount of urea would render an increase in the SSAs for the samples. Kim et al. [36] also reported that ceria-zirconia mixed oxides prepared by the continuous hydrothermal method exhibited higher SSAs, nearly 1.5–2.0 times of the ones synthesised by coprecipitation. In addition, it was also found that the presence of 0.10 wt% Ru had little influence on the SSAs of hydrothermally prepared CZ samples, whilst it decreased the SSAs of coprecipitated CZ sample. This phenomenon could be associated with the incorporation of Ru into the structure of the coprecipitated CZ sample, corresponding with the increased mean pore size from 86 to 98 nm and the decreased SSA from 26 to 18 m^2/g. On the other hand, there were no significant changes observed for Ru-impregnated hydrothermally prepared CZ samples regarding the total pore volume and mean pore size. This observation might be resulted from different synthesis processes as Álvarez Moreno et al. [37] also found that the synthesis process can affect the dispersion of noble metals on the materials, further leading to either the increase or decrease in the values of surface area, pore volume and pore size of the materials. Furthermore, it is consistent with the finding of Lyu et al. [38] who studied four different synthesis methods, i.e., dry impregnation, strong electrostatic adsorption, coprecipitation and combustion synthesis, on dry reforming of methane with a combination of $Ni/Ce_xZr_{1-x}O_2$. They observed that when the loading amount of Ni was increased from 2 wt% to 10 wt%, the SSA decreased to the lowest one among all the samples prepared by other methods, around 30% less surface area and 40% less pore volume. Therefore, the preparation method appears to be critical to optimise the textural properties of the materials for the maximum catalytic performance. In this study, hydrothermal method exhibited advantages over coprecipitation on the textural stability.

Fig. 1 shows the XRD patterns of all the samples, and their characteristic values (crystallite size and lattice parameters) extracted from the diffractograms are presented in Table 2. It was found that the introduction of Ru and Zr did not change the diffraction peaks of CeO_2 at $2\theta = 28.6°$, 33.2°, 47.7°, and 56.4°, which corresponded to (111), (200), (220), and (311) planes, respectively. These results suggested that the crystallinity of CeO_2 was preserved in the presence of Ru and Zr. In addition, these peaks are also in line with the characteristic peaks of Ce75Zr25 (Fig. S2). A broader and more intense diffraction peak was subsequently observed after increasing the molar ratio of CZ to U from 1:2 to 1:5. This change was believed to be resulted from the formation of smaller particles with smaller crystallite size (120 °C: 17.3 to 8.8 nm; 180 °C: 14.2 to 8.8 nm) when a higher amount of urea was used. The larger SSA as shown in Table 2 can also support this observation. However, the variables of the hydrothermal reaction temperatures and the ratio of CZ to U had no effects on the Bragg peak position, and then the crystalline structures and lattice parameters, as shown in Table 2. Moreover, Ru was found to impart insignificant effect on the crystallinity of the CZ samples irrespective of the synthesis method, i.e., coprecipitation and hydrothermal method in this study. This could possibly be ascribed to two reasons: i) the very low amount of Ru (0.10 wt%) impregnated on these samples, below the detection limit of laboratory XRD instrument, thus giving rise to little diffraction; and ii) the high dispersion of Ru on the CZ samples could participate in the CZ lattice structure, which subsequently created the Ru–Ce–O bonds [39]. Only then, XRD would display the main structure of CeO_2. Structural analyses by SEM will be presented in the next section, confirming the presence of highly dispersed state of Ru on the CZ samples.

Morphological properties of hydrothermal synthesised ceria-zirconia oxides

The SEM images of CZ samples are shown in Fig. 2. A clear distinction was observed when the concentration of urea was increased, that a spherical structure was developed for 1CZ5U-120 compared to the "fan-shaped" 1CZ2U-120. It is also noteworthy that with the increasing hydrothermal reaction temperature on 1CZ2U, nanorodic structure became

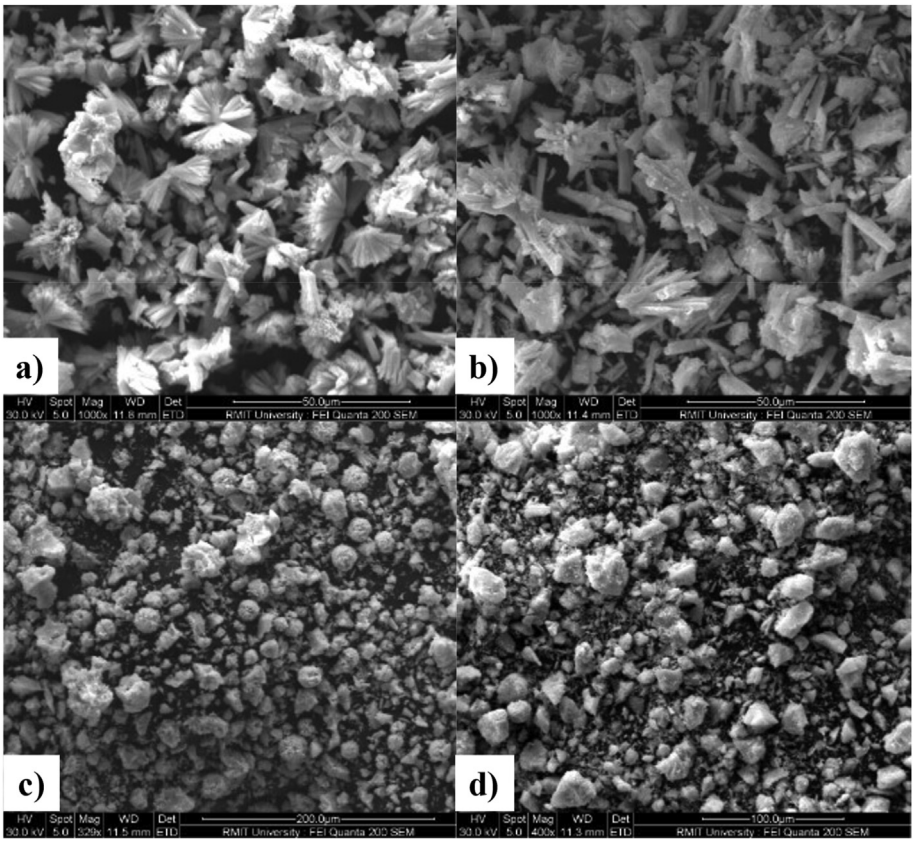


Fig. 2 – FE-SEM micrographs of a) 1CZ2U-120, b) 1CZ2U-180, c) 1CZ5U-120, d) 1CZ5U-180).

dominated in 1CZ2U samples [Fig. 2 (b)]. This observation could be associated with the sharp peaks (200) and (220) observed from XRD in Fig. 1. Based on these results, it can be concluded that increases in urea concentration and hydrothermal reaction temperature favoured the formation of smaller CZ particle. This might be due to an accelerated hydrolysis and crystallisation with the latter evidenced from the smaller crystallite size as confirmed by XRD measurement (Table 2). Mai et al. [40] demonstrated that by increasing the concentration of NaOH during a hydrothermal synthesis, it was possible to vary the shape of ceria from polyhedral to rods. In addition, increasing the temperature of hydrothermal reaction from 100 °C to 180 °C, the shape of ceria nanoparticles was changed from rods to cubes. In this study, CZ samples at 120 °C also exhibited the dominance of nanorods but shaped in "fan" and/or "sphere" [seen in Fig. S3 (a) and Fig. S3 (c)]. Kunudom et al. [41] recently reported that nanocubes of $Ce_{0.75}Zr_{0.25}O_2$ with well-exposed crystalline plane (100) would be formed under a high concentration of NaOH (7.5 M) at a hydrothermal reaction temperature of 200 °C. They also revealed that planes of (100) and (110) in CZ materials were more catalytically active for the steam reforming of AcOH and showed higher resistance against deactivation by coke. This finding is consistent with our study that nanorodic/cubic structures (1CZ5U-120 and 1CZ5U-180) presented better catalytic activities in the later section. In contrast, Ce75Zr25 prepared by coprecipitation was dominated with cubes and parallelepiped [shown in Fig. S3 (e) and (f)] but poorly performed in catalytic activity, which might be due to the synthesis route.

Reducibility studies

The reducibility and the OSC of the CZ samples and Ru-impregnated CZ samples were investigated by using H_2-TPR. Fig. 3 shows the reduction behaviours of all the samples, represented by the differential weight change plotted against reduction temperature. Their corresponding calculated OSC results are summarised in Table 3 as the amount of oxygen removed from 50 °C to the various cut-off temperatures.

Fig. 3 (a) shows that CZ samples exhibited three distinct reduction peaks in the temperature range of 200–410 °C (Peak I centred at 310 °C), 410–670 °C (Peak II centred at 556 °C) and 670–900 °C (Peak III centred at 860 °C). As reported in the literature [42–44], Peak I and Peak II are ascribed to the reduction of surface oxygen groups, while Peak III is resulted from the reduction of subsurface or bulk oxygens [43]. Upon increasing the hydrothermal reaction temperature from 120 °C to 180 °C, the characteristic reduction temperatures of Peak I and Peak III were shifted slightly to a lower temperature. The observed shift was also accompanied with the increased OSC from 1246 (1CZ2U-120) μmol·O/g-cat to 1523 (1CZ2U-180) μmol·O/g-cat and from 1698 (1CZ5U-120) μmol·O/g-cat to 1784 (1CZ5U-180) μmol·O/g-cat, respectively (Table 3). This decrease in reduction temperature with the increase in OSC was indicative of the formation of more easily

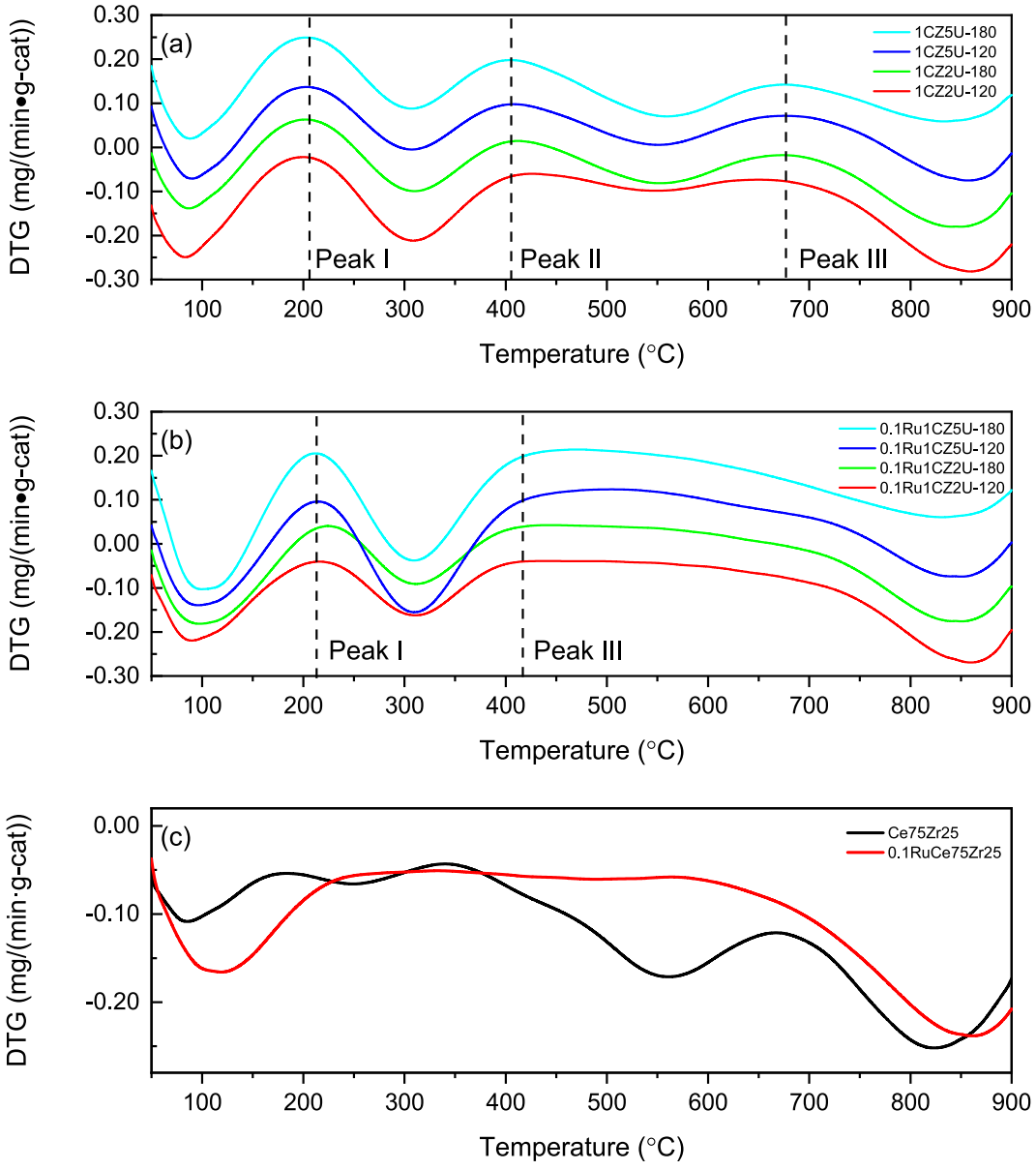


Fig. 3 – DTG curves of CZ samples (a), Ru-impregnated CZ samples (b), Ce75Zr25 and 0.1RuCe75Zr25 (c) in the temperature range of 50 °C–900 °C with the heating rate of 5 °C/min under 4% H_2/Ar.

Table 3 – OSC (μmol·O/g-cat) of catalysts measured at different cut-off temperatures.

Temp./°C	400	500	600	700	750	800	850
1CZ2U-120	578	673	788	877	882	1057	1246
1CZ2U-180	599	766	973	1172	1226	1392	1523
1CZ5U-120	704	841	1131	1243	1344	1501	1698
1CZ5U-180	760	941	1219	1400	1480	1621	1784
0.1Ru1CZ2U-120	578	583	649	721	792	847	1073
0.1Ru1CZ2U-180	790	800	899	1028	1068	1252	1431
0.1Ru1CZ5U-120	1153	1194	1390	1503	1592	1693	1925
0.1Ru1CZ5U-180	1172	1177	1333	1505	1625	1776	1922
Ce75Zr25	248	371	574	720	810	985	1148
0.1RuCe75Zr25	389	458	539	657	727	824	991

exchangeable oxygen groups in the catalyst system. This could be caused by the formation of varying structural defects in CZ samples under different hydrothermal conditions, mainly derived from the ionic radii of Ce^{3+} and Ce^{4+}. Larger number of structural defects could provide high concentration of oxygen vacancies, which in turn increased the oxygen mobility [45]. Likewise, the increase of the ratio of CZ to U also saw an increasing amount of OSC, corresponding to a larger extent of reduction of Peak II.

On the other hand, Ru-impregnated CZ samples also exhibited a similar reduction profile but only revealed two major reduction peaks over the temperature range as shown in Fig. 3 (b). There was no single broad reduction peak observed in the temperature region of 410–670 °C compared to the bare CZ samples. Meanwhile, Peak I became more pronounced and represented with the increased oxygen storage/exchange capacity. This capability increase is likely to be associated with the promoted oxygen exchange capability by introducing Ru to CZ samples [43]. This would be attributed to the improved oxygen spillover in the presence of Ru. As reported, when Ru was present, the combination of Ru and supports could be reduced at low temperatures below 270 °C [43,46]. It was because the occurrence of low-temperature ruthenium oxide reduction facilitated the overall catalyst reduction by the improved interactions with supports. As a result, the more exchangeable oxygens became available, especially in the low temperature range of 400–600 °C. These results are summarised in Table 3. As such, the amount of OSC increased from 760 μmol·O/g-cat (1CZ5U-180) to 1172 μmol·O/g-cat (0.1Ru1CZ5U-180) at 400 °C, which is approximately 1.5 times higher when Ru was present. This result thus demonstrated that the presence of trace amounts of Ru could enhance the oxygen spillover effect over the hydrothermally prepared CZ samples.

Fig. 3 (c) illustrated the pronounced difference in the reduction profiles of Ce75Zr25 and 0.1RuCe75Zr25 over the studied temperature range. The presence of Ru saw a significant decrease in the surface reduction temperature from 550 °C to 120 °C. As discussed earlier, the reduction in temperature was likely due to the close interaction between Ru and CZ support, leading to the lower temperature of reduction observed at 120 °C. Apparently, coprecipitation and hydrothermal synthesis methods led to the formation of different structures of CZ supports at the surface, which interacted with Ru differently. Consequently, the reduction took place to a lesser extent at the low-temperature regime (<400 °C) for the coprecipitated CZ sample. This observation was attributed to the fewer exchangeable oxygens exposed in coprecipitated CZ supports at low temperatures in the presence of Ru compared to the hydrothermally synthesised CZ samples. The higher number of exchangeable oxygens in hydrothermally prepared CZ supports in turn increased the oxygen mobility, which is recognised as the main driver for the enhancement of catalytic activity and the higher carbon resistance to be discussed in Section Catalytic activities for dry reforming of methane [47–50].

In the study, these OSC values of all the samples that are tabulated in Table 3 increased with increasing cut-off temperature. It is suggested that the exchange of oxygen between the surface and the bulk is an endothermic process, therefore increasing the temperature would favour the transport of oxygen and increase the kinetics of the process. This finding is in agreement with an early report by Bedrane et al. [51] who found that bulk diffusion was as a function of reaction temperature and responsible for a large increase of OSC. In our work, despite the trace amount of Ru, its presence could significantly increase the OSC up to 1.5 times than that of the bare CZ samples. This increment could be attributed to the changes in Peak I and Peak II as displayed in Fig. 3 (b). In addition, the increased amount in oxygen removal and thus the reducibility suggested that the oxygen exchangeable process involved in not only surface oxygen but also lattice oxygen particularly at lower temperatures, compared to the bare CZ samples. The latter could involve the transfer of oxygen across the concentration gradient in the bulk to the surface of the CZ support. Liu et al. [52] reported similar results and found that the greater degree of low-temperature oxygen reduction produced more available reactive oxygen species at the surface, which subsequently enhanced the performance of ceria-based materials in their study. They also highlighted the importance of oxygen vacancies in facilitating the formation and transportation of other secondary active oxygen species. On the other hand, Rocchini et al. [53] demonstrated a positive effect of oxygen exchange capability on the redox behaviours and the promoting effect of oxygen spill-over from the sub-surface structure to the surface in the presence of noble metals. Furthermore, Li et al. [54] found that different synthesis approaches could lead to different degrees of oxygen defects. Their finding suggested that the larger degree of oxygen defects the higher oxygen mobility and better reducibility. It is noteworthy that for those CZ samples under current investigation, the incorporation of Zr into CeO_2 effectively increased the dispersion of doping metals, i.e., Ru, and the degree of metal-support interaction, and further increased the number of lattice oxygen species and OSC values [47]. As a result, the oxygen exchange was facilitated and the reducibility at low temperature was improved, thereby leading to the improved catalytic performance of DRM.

Catalytic activities for dry reforming of methane

The catalytic activities of CZ and Ru-impregnated CZ samples for DRM as a function of reaction temperature are shown in Fig. 4. The conversions of CH_4 and CO_2 increased with the reaction temperature, on account of the nature of DRM's endothermicity. CO_2 conversions were always found to be higher than that of CH_4 over the studied temperature range. This discrepancy could be attributed to the occurrence of reverse water gas shift reaction (RWGS) where an additional amount of CO_2 was consumed with the produced H_2 to form CO and H_2O. However, the effect of RWGS on CO_2 consumption diminished from 13.4% at 600 °C to approximately 2% at a temperature of 850 °C. It was therefore evident that the ratio of H_2 to CO was lower than the stoichiometric value of 1.0.

Fig. 4 shows that bare CZ samples exhibited relatively higher onset reaction temperatures for CH_4 and CO_2 conversions. That is, CH_4 conversion started to take place from 600 °C for bare CZ samples; however, this temperature was lowered to 400 °C for Ru-impregnated CZ samples. Likewise, CO_2 conversion became noticeable at 500 °C and 400 °C for bare CZ

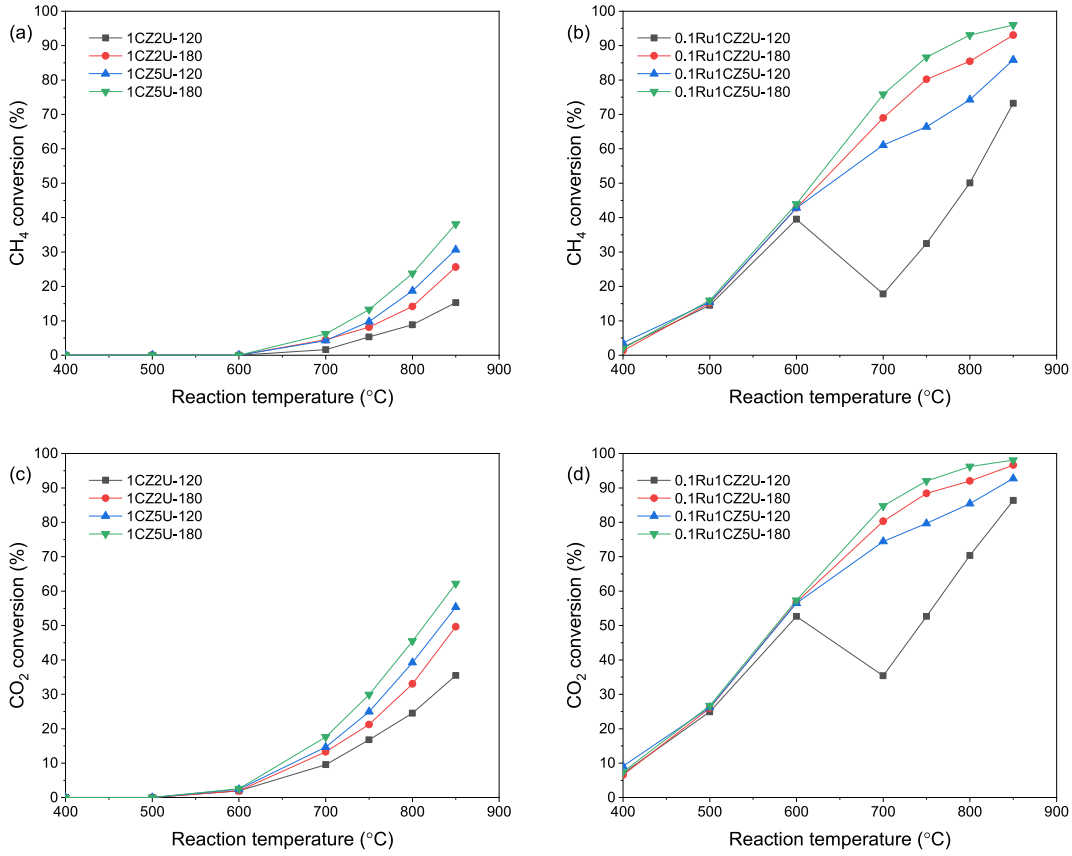


Fig. 4 – Catalytic performance of CZ samples and Ru-impregnated CZ samples in DRM, CH_4 conversions (a) (b) and CO_2 conversions (c) (d).

samples and Ru-impregnated CZ samples, respectively. Based on the results in Fig. 3, the oxygen vacancies at the catalyst surface, i.e., on ceria-zirconia surface, were deemed to be the catalytic sites. As the number of oxygen vacancies and the spillover of oxygen were enhanced in the presence of Ru, the conversions of both CH_4 and CO_2 thus became more favourable particularly at the lower temperature spectrum in this study. Rossignol et al. [55] revealed that the reduction profiles of $Zr_{1-x}Ce_xO_2$ mixed oxides could be varied with the synthesis methods with a greater degree of reduction at higher oxygen mobility and OSC values. As mentioned above, high oxygen mobility is responsible for enhancing the overall catalytic activity and carbon resistance. To our best knowledge, there is a lack of literature that highlighted the significant effect of a small amount of Ru (as low as 0.10 wt%) on ceria-zirconia on dry reforming of methane in the temperature region of 400–850 °C.

For clarity, the catalytic activities of CZ materials in this study were considered at the low temperature region (400 °C–600 °C) and the high temperature region (700 °C–850 °C). In view of the literature, limited number of successes have been reported in producing an active DRM catalyst in the low temperature region which is of great interest in this study. In the low temperature range, there was hardly any noticeable conversions of CH_4 and CO_2 on bare CZ samples due to the thermodynamic limitations. However, as soon as 0.10 wt% Ru was introduced onto CZ samples, a significant improvement on the DRM activity was observed. Particular attention should be paid to 0.1Ru1CZ5U-180 where this catalyst achieved CH_4 and CO_2 conversions up to 44.0% and 57.4%, respectively, at a temperature of 600 °C. This significant improvement in low temperature catalytic activity could be ascribed to the increased amount of oxygen vacancies and oxygen mobility as evidenced by the observed high degree of reduction shown in Fig. 3. In addition, no carbon was detected on the surface of the used catalyst after the reaction. This result agreed with the theoretical thermodynamic equilibrium values calculated using HSC chemistry software performed for the current system containing 41% CH_4 and 54% CO_2. A collection of similar research works was further recorded in Table 4 to validate that our results were outperformed in terms of that trace amounts of Ru employed for dry reforming of methane at such low temperature of 600 °C.

Besides, it is well-established that under the conditions of DRM, carbon formation is highly favourable in the temperature range of 546–703 °C due to the co-occurrence of CH_4 decomposition and CO disproportionation reaction [61]. From our carbon balance calculations and post-reaction carbon analyses, no carbonaceous species was detected on the catalyst after DRM reaction at 600 °C [Fig. 5 (b)]. Several studies also revealed that the introduction of Ru could reduce the carbon formation due to the high reforming activity of Ru and the relative low carbon growth rates on Ru surface [43,62].

Table 4 – A collection of research works on low-temperature dry reforming of methane over ceria-zirconia support and/or small noble metal loadings.

Samples	Temp. (°C)	Feedstock CO_2/CH_4	Methods	Conversions (%)		Carbon formed	Ref.
				CH_4	CO_2		
10 wt% $Ni/Ce_{0.62}Zr_{0.38}O_2$	550	1	Experimental	39	39	Yes	[56]
5 wt% $Ni/Ce_{0.6}Zr_{0.34}O_2$	600	1	Experimental	35	51	Yes	[57]
4 wt% Ru/ZrO_2–La_2O_3	600	1	Experimental + Theoretical	60	70	–	[58]
–	600	1.5	Theoretical	54	49	Yes	[59]
RhNi–$MgAl_2O_4$ (0.6 wt%Rh)	600	1	Experimental	43	52	Negligible	[60]
Ru–Ni–Mg-CZO (0.16 wt% and 0.32 wt%)	450	1	Experimental	4	9	Negligible	[24]

However, in most cases, there was a need to use high loadings of Ru, usually at a level between 2 wt% and 5 wt%. In contrast, this study has shown that the use of a relatively lower loading of Ru at 0.10 wt% in conjunction with ceria-zirconia supports, could efficiently suppress carbon formation and at the same time achieve high conversions of CH_4 and CO_2. The observed enhancement in low temperature activity is attributed to the facilitated oxygen exchanging process from the bulk to the surface in the presence of Ru.

It has been proposed that two main reactions were dominated on the surface of Ru-impregnated CZ samples during DRM [63]. Herein, oxygen vacancies in CZ samples are playing a critical role in reducing CO_2 and further facilitate oxidising CH_4 to syngas [64,65]. As indicated by Eq. (8), the reaction involves the conversion of CH_4 into CO and H_2; whereas Eq. (7) showed that oxygen vacancies render CO_2 to be reduced to CO and lattice oxygen (O_M). Additionally, having the ability to store and release oxygen in its lattice, ceria can produce active oxygens to oxidise carbonaceous species adsorbed on the surface [66]. The oxidation of carbon by active surface oxygen species [Eq. (9)] has been reported as an inverse relationship with carbon formation [38,67]. The number of active oxygens was dependent on the degree of oxygen defects in the CZ samples and the oxygen exchanging rate from the bulk to the surface. The trace amounts of Ru therefore facilitated oxygen exchange which then improved the catalytic activity of DRM as well as suppressed coke formation.

$$O_v + CO_2 \rightarrow O_M + CO \quad (7)$$

$$O_M + CH_4 \xrightarrow{Ru} CO + 2H_2 \quad (8)$$

$$O_M + C \xrightarrow{Ru} CO \quad (9)$$

This promotional effect of Ru continued into the high temperature range. 0.1Ru1CZ5U-180 was also found to be highly catalytically active in the high temperature region, achieving conversions up to 96% for CH_4 and 98% for CO_2 at 850 °C (Fig. 4). One of the major driving forces for the observed high conversions was the fact that the kinetics of endothermic DRM is much faster at high temperatures. However, a decrement in conversion was observed for 0.1Ru1CZ2U-120 at 700 °C (Fig. 4), which could be due to the formation of the segregated ZrO_2 phase, as evidenced from the XRD analysis that did not contribute to any improved oxygen storage and would cover the active sites on the catalyst surface (Fig. S4). Secondly, the oxygen spillover process was promoted by Ru, which in turn improved both the mobility of oxygen, and the oxygen exchanges between the adsorbed species and the catalyst surface. The combined effect gave rise to the observed high catalytic activity. Moreover, the close interaction of Ru with CZ support prepared by the hydrothermal method provided an effective pathway for oxygen to be transported between Ru surface and assisted the migration of oxygen from CZ lattice to CZ surface. Thirdly, the increase in the specific surface area and the reduction in crystallite size (Table 1) would also contribute to the improved catalytic performance [47]. Based on the preliminary optimisation studies of the Ru loading, it was found that even trace amounts of Ru are sufficient to provide high oxygen exchanging capability and catalytic activity for DRM. As shown in Fig. 5.1Ru1CZ5U-180 showed stable catalytic activity of DRM without noticeable changes in the 2-h reforming reaction. All these results suggest that the dynamics of oxygen exchange between the adsorbed species and the surface of CZ could be perturbed significantly by the presence of surface metal and the method of synthesising the base CZ materials. In view of the literature, there are only a limited number of studies on using metal catalysts at such low loadings. Whang et al. [68] reported that high catalytic activity of DRM (86.6% CH_4 and 98.8% CO_2) at 800 °C were achieved by loading a small amount of Ru (0.13 wt %) on ZrO_2–SiO_2. They also found that the catalytic activity of this type of catalysts remained stable for up to 20 h, and Ru was the primary catalytically active sites which were responsible for their observed high catalytic activity. Unfortunately, no low-temperature catalytic activity was reported by the authors. On the other hand, Kamiuchi et al. [69] pointed out that small Pt loadings (0.001 wt%) could assist the release of oxygen from CZ supports when these materials were used for the catalytic oxidation of CO.

As a comparison, Ce75Zr25, 0.1RuCe75Zr25 and 0.1NiCe75Zr25 prepared by the conventional coprecipitation method were benchmarked with the hydrothermally synthesised samples. As shown in Fig. 6, all coprecipitated CZ samples yield lower conversions of CH_4 and CO_2 in the low temperature region. Similar to the results obtained from the hydrothermally synthesised samples, the presence of a trace amount of Ru (0.10 wt%) significantly improved the catalytic conversions of CH_4 and CO_2 between 400 °C and 850 °C. On the other hand, the presence of Ni only had a slightly positive impact on the catalytic performance in contrast to base Ce75Zr25. When the reaction temperature was increased, the promoting effect of Ru became more pronounced, especially at temperatures over 600 °C. A small yet noticeable decrease in

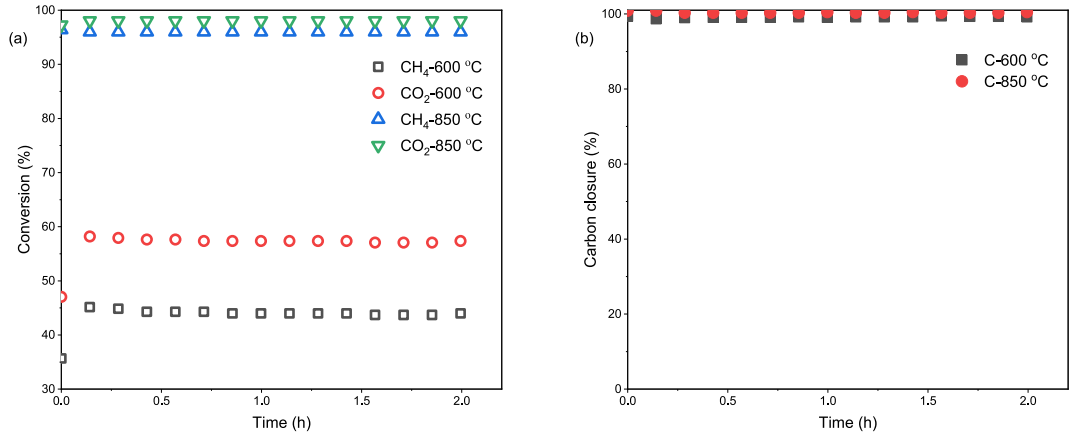


Fig. 5 – (a) CH_4 and CO_2 conversion as a function of time on stream under two different reaction temperatures for 0.1Ru1CZ5U-180; (b) carbon closure at 600 °C and 850 °C for 2 h time-on-stream for 0.1Ru1CZ5U-180.

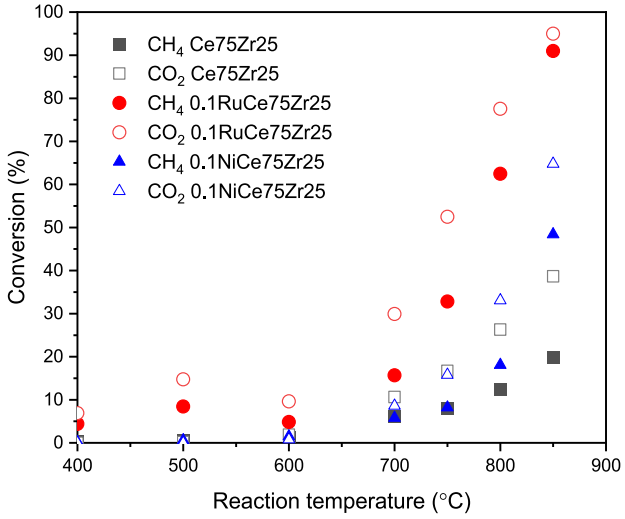


Fig. 6 – Catalytic performance of Ce75Zr25, 0.1RuCe75Zr25 and 0.1NiCe75Zr25 in DRM.

CH_4 and CO_2 conversions for 0.1RuCe75Zr25 was observed at 600 °C in the first hour. However, the reaction rate stabilised to a steady level afterwards as shown in Figs. 6 and 7 (a). It is likely due to the carbon formed during the reforming reaction which corresponded to the first half-an-hour decrease in carbon closure shown in Fig. 7 (b). In addition, because all the samples were calcined at 650 °C, as soon as the reaction temperature was near or higher than the calcination temperature, a re-stabilisation of CZ materials took place. As the reaction proceeded, a more thermally stable structure was developed. Considering the steady state conversions of CH_4 and CO_2, these values were five times lower than those of 0.1Ru1CZ5U-180 (44.0% and 57.4%). This large difference was likely due to the different structures of base CZ supports prepared by coprecipitation and hydrothermal method, especially the exposed crystalline phases. The hydrothermally prepared CZ supports displayed no diffraction of (110) phase upon XRD analysis (seen in Fig. 1 and Fig. S2). It is clear that the catalyst synthesis methods strongly influenced on the

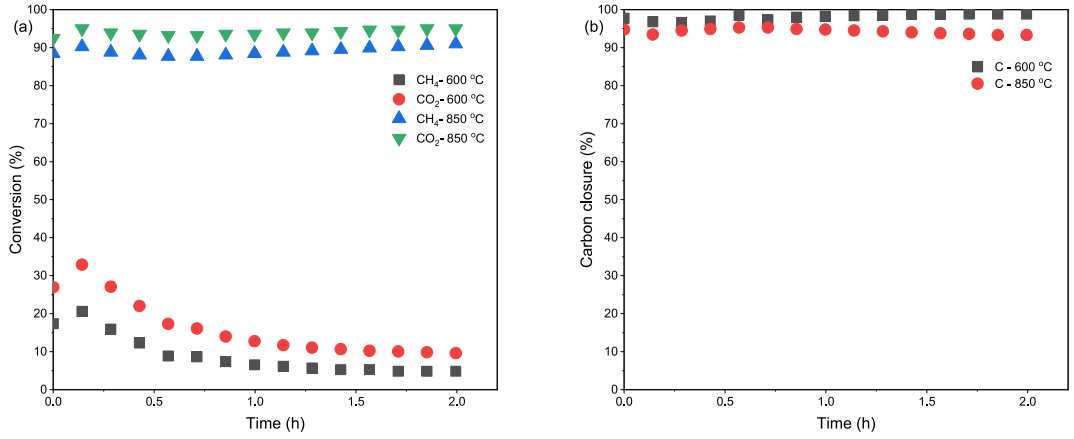


Fig. 7 – (a) CH_4 and CO_2 conversion as a function of time on stream under two different reaction temperatures for 0.1RuCe75Zr25; (b) carbon closure at 600 °C and 850 °C for 2 h time-on-stream for 0.1RuCe75Zr25.

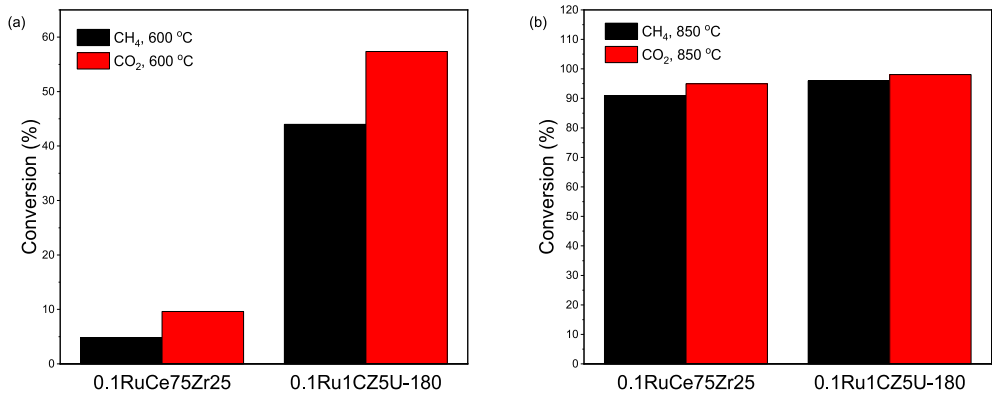


Fig. 8 – Catalytic activities at 600 °C (a) and 850 °C (b) for 0.1Ru1CZ5U-180 and 0.1RuCe75Zr25.

structure-activity relationship as the synthesis methods alter the structure, texture and surface properties of the CZ materials as well as the degree of oxygen defects induced [54,55]. The higher degree of oxygen defects, observed with the separated ZrO_2 from Ru-CZ after DRM reaction, in Fig. S4, provided more active sites for high catalytic activities of DRM.

As the reaction temperature increased further, 0.1RuCe75Zr25 achieved high conversions of CH_4 and CO_2, obtaining 91% and 95%, respectively. The carbon closure at 850 °C for 0.1RuCe75Zr25 was found to be around 95%. This small yet noticeable deviation from 100% carbon closure was likely considered as the loss of carbon in the gas phase and the formation of carbon deposits during the reaction. On the contrary, no detectable change was observed for 0.1Ru1CZ5U-180 under the same conditions [Fig. 5 (b)]. Although no catalyst deactivation was observed after 2 h of reaction at 850 °C, the loss of carbon was likely attributed to the formation of different carbonaceous species, such as amorphous carbon. As for the variation at 600 °C, the loss of catalytic activity might be because of insufficient oxygen exchanging capability in DRM reaction. Low OSC values of 0.1RuCe75Zr25 compared to that of 0.1Ru1CZ5U-180 in Table 2 suggests that oxygens available for DRM could not be replenished as quickly as it generated along the reaction, despite the presence of Ru. Fig. 8 clearly shows a distinct difference between coprecipitation and the hydrothermal method on the catalytic performance, especially at low temperature (600 °C). All these results furthermore highlighted the importance of structures of base CZ supports on DRM reaction.

To further establish the structure-activity relationship, the morphologies of coprecipitated and hydrothermal samples were compared and correlated to the catalytic activity. It was found that the parallelepiped shape [Fig. S3 (e)] was dominated in the samples prepared by coprecipitation (Ce75Zr25) while spherical and/or bouquet-like structures dominated in the hydrothermally synthesised CZ samples. This observation suggested that preferential indexes of the samples would be exposed for DRM reaction, varying with the synthesis methods (Fig. S3 and Fig. S4). Balducci et al. [22] found that lattice decrease in CZ samples reduced the reduction energy on the stable (110) and (111) phases, which subsequently made the bulk oxygen more susceptible for reduction. As such, higher OESC and more exchangeable oxygens in the lattice were obtained. Besides, smaller SSA (Table 1) was observed in coprecipitated CZ sample, suggesting that the same amount of Ru might not be able to disperse well in order to supply sufficient oxygen exchanging for DRM reaction. On the other hand, hydrothermally synthesised CZ samples provided relatively larger SSAs for Ru dispersal. Moreover, there was a segregated CeO_2 and ZrO_2 phases after DRM reaction as shown in Fig. S4. As a result, the structural defects would evolve, thereby producing more exchangeable oxygens in the lattice. Li et al. [54] revealed that ceria-zirconia prepared by a new complexing-coprecipitation method could expose t"-phase with rich oxygen defects, excellent bulk oxygen migration and redox abilities than the samples prepared by other methods. Fig. S5 presents a preliminary synchrotron XRD result that during the DRM reaction, intensity of crystalline phases of coprecipitated CZ sample slightly decreased with increasing the reaction temperature (excluding lattice expansion due to the increasing temperature). However, the hydrothermally synthesised CZ sample gave rise to the intensity of crystalline phases after switching to reactive gas (5 vol%CH_4/5 vol% CO_2/Ar). In the presence of excess urea adopted in this study, the hydrothermal synthesis method has the advantage to provide CZ materials with more active oxygen species for DRM reaction.

Conclusion

In this study, two different methods were employed to prepare bare CZ samples, i.e., hydrothermal method and coprecipitation. Ru was introduced by the wetness impregnation. All samples were examined with the DRM reaction in the temperature range of 400–850 °C. The effects of hydrothermal operational conditions were studied and found that the higher concentration of urea and hydrothermal reaction temperature can enable higher catalytic conversions of CH_4 and CO_2 in the temperature range of interest. Notably, the presence of noble metal Ru significantly improved the low-temperature DRM activity compared to bare CZ samples. This enhancement could be ascribed to the increased number of oxygen vacancies at all temperatures and high oxygen mobility, which is likely to correlate to a greater extent of structural defects and fast lattice oxygen diffusion. 0.1Ru1CZ5U-180 was the

optimum catalyst for low-temperature and high-temperature catalytic conversions and stability of both CH_4 and CO_2. This was because higher specific surface area warranted a well-dispersion of Ru which is considered to be the active sites for DRM reaction and is the entity that mobilise lattice oxygen from the bulk to the surface. It has achieved up to 44.0% and 57.4% at 600 °C, 96% and 98% at 850 °C for CH_4 and CO_2, respectively. This low-temperature conversion was close to the values calculated from the thermodynamic equilibrium conditions. It could be the result of less carbon accumulated during the testing period of time. More importantly, a structure-activity relationship was developed in the presence of a very small loading amount of Ru (0.10 wt%), the more spherical the higher catalytic activity of DRM.

Declaration of competing interest

The authors declare that they have no known competing financial interests or personal relationships that could have appeared to influence the work reported in this paper.

Appendix A. Supplementary data

Supplementary data to this article can be found online at https://doi.org/10.1016/j.ijhydene.2023.07.079.

REFERENCES

[1] Ross JRH, van Keulen ANJ, Hegarty MES, Seshan K. The catalytic conversion of natural gas to useful products. Catal Today 1996;30:193–9.

[2] El-Nagar RA, Ghanem AA. Syngas production, properties, and its importance. In: Sustainable alternative syngas fuel. IntechOpen; 2019.

[3] Julbe A, Guizard C. Role of membranes and membrane reactors in the hydrogen supply of fuel cells. Ann Chim-Sci Mat 2001;26:79–92.

[4] Simakov DSA, Román-Leshkov Y. Highly efficient methane reforming over a low-loading Ru/γ-Al2O3 catalyst in a Pd-Ag membrane reactor. AIChE J 2018;64:3101–8.

[5] Al–Swai BM, Osman NB, Ramli A, Abdullah B, Farooqi AS, Ayodele BV, et al. Low-temperature catalytic conversion of greenhouse gases (CO2 and CH4) to syngas over ceria-magnesia mixed oxide supported nickel catalysts. Int J Hydrogen Energy 2021;46:24768–80.

[6] Aitbekova A, Wu L, Wrasman CJ, Boubnov A, Hoffman AS, Goodman ED, Bare SR, Cargnello M. Low-temperature restructuring of CeO2-supported Ru nanoparticles determines selectivity in CO2 catalytic reduction. J Am Chem Soc 2018;140:13736–45.

[7] Elsayed NH, Roberts NRM, Joseph B, Kuhn JN. Low temperature dry reforming of methane over Pt–Ni–Mg/ceria–zirconia catalysts. Appl Catal B Environ 2015;179:213–9.

[8] Wang Y, Yao L, Wang Y, Wang S, Zhao Q, Mao D, Hu C. Low-temperature catalytic CO2 dry reforming of methane on Ni-Si/ZrO2 catalyst. ACS Catal 2018;8:6495–506.

[9] Liu Z, Zhang F, Rui N, Li X, Lin L, Betancourt LE, Su D, Xu W, Cen J, Attenkofer K, Idriss H, Rodriguez JA, Senanayake SD. Highly active ceria-supported Ru catalyst for the dry reforming of methane: in situ identification of Ruδ+–Ce3+ interactions for enhanced conversion. ACS Catal 2019;9:3349–59.

[10] Singha RK, Yadav A, Shukla A, Kumar M, Bal R. Low temperature dry reforming of methane over Pd-CeO2 nanocatalyst. Catal Commun 2017;92:19–22.

[11] Wang S, Lu GQ, Millar GJ. Carbon dioxide reforming of methane to produce synthesis gas over metal-supported catalysts: state of the art. Energy Fuel 1996;10:896–904.

[12] Zhang S, Muratsugu S, Ishiguro N, Tada M. Ceria-Doped Ni/SBA-16 catalysts for dry reforming of methane. ACS Catal 2013;3:1855–64.

[13] Valderrama G, Urbina de Navarro C, Goldwasser MR. CO2 reforming of CH4 over Co–La-based perovskite-type catalyst precursors. J Power Sources 2013;234:31–7.

[14] Kumar P, Sun Y, Idem RO. Nickel-based ceria, zirconia, and ceria–zirconia catalytic systems for low-temperature carbon dioxide reforming of methane. Energy Fuel 2007;21:3113–23.

[15] Yamaguchi D, Tang L, Scarlett N, Chiang K. The activation and conversion of carbon dioxide on the surface of zirconia-promoted ceria oxides. Chem Eng Sci 2020;217:115520.

[16] Sun J, Yamaguchi D, Tang L, Periasamy S, Ma H, Hart JN, Chiang K. Enhancement of oxygen exchanging capability by loading a small amount of ruthenium over ceria-zirconia on dry reforming of methane. Adv Powder Technol 2022;33:103407.

[17] Boaro M, Colussi S, Trovarelli A. Ceria-based materials in hydrogenation and reforming reactions for CO2 valorization. Front Chem 2019;7:28.

[18] Wang F, Li C, Zhang X, Wei M, Evans DG, Duan X. Catalytic behavior of supported Ru nanoparticles on the {100}, {110}, and {111} facet of CeO2. J Catal 2015;329:177–86.

[19] Kovacevic M, Mojet BL, van Ommen JG, Lefferts L. Effects of morphology of cerium oxide catalysts for reverse water gas shift reaction. Catal Lett 2016;146:770–7.

[20] Violi IL, Zelcer A, Bruno MM, Luca V, Soler-Illia GJAA. Gold nanoparticles supported in zirconia–ceria mesoporous thin films: a highly active reusable heterogeneous nanocatalyst. ACS Appl Mater Interfaces 2015;7:1114–21.

[21] Dong F, Tanabe T, Takahashi N, Shinjoh H. Investigation of the effective oxygen storage and release performances on the Pt/CeO2-ZrO2 catalysts by breakthrough method. Catal Today 2019;332:259–66.

[22] Balducci G, Kašpar J, Fornasiero P, Graziani M, Islam MS. Surface and reduction energetics of the CeO2–ZrO2 catalysts. J Phys Chem B 1998;102:557–61.

[23] Whang HS, Choi MS, Lim J, Kim C, Heo I, Chang TS, Lee H. Enhanced activity and durability of Ru catalyst dispersed on zirconia for dry reforming of methane. Catal Today 2017;293:122–8.

[24] Sokefun YO, Trottier J, Yung MM, Joseph B, Kuhn JN. Low temperature dry reforming of methane using Ru-Ni-Mg/ceria-zirconia catalysts: effect of Ru loading and reduction temperature. Appl Catal a-Gen 2022:645.

[25] Chen J, Yao C, Zhao Y, Jia P. Synthesis gas production from dry reforming of methane over Ce0.75Zr0.25O2-supported Ru catalysts. Int J Hydrogen Energy 2010;35:1630–42.

[26] de Leitenburg C, Trovarelli A, Llorca J, Cavani F, Bini G. The effect of doping CeO2 with zirconium in the oxidation of isobutane. Appl Catal Gen 1996;139:161–73.

[27] Nagarajan VS, Rao KJ. Characterization of sol-gel derived zirconia with additions of yttria and ceria. Origin of high fracture toughness in ceria-stabilized samples. Philos Mag A 1992;65:771–81.

[28] Chen YL, Qi M, Yang DZ, Wu KH. Mechanical alloying of ceramics in zirconia-ceria system. Mater Sci Eng, A 1994;183:L9–12.

[29] Stark WJ, Maciejewski M, Mädler L, Pratsinis SE, Baiker A. Flame-made nanocrystalline ceria/zirconia: structural

properties and dynamic oxygen exchange capacity. J Catal 2003;220:35–43.
[30] Ozawa M, Kimura M, Isogai A. The application of Ce Zr oxide solid solution to oxygen storage promoters in automotive catalysts. J Alloys Compd 1993;193:73–5.
[31] Hirano M, Miwa T, Inagaki M. Low-temperature direct synthesis of nanoparticles of fluorite-type ceria–zirconia solid solutions by "forced cohydrolysis" at 100°C. J Solid State Chem 2001;158:112–7.
[32] Machmudah S, Widiyastuti W, Wahyudiono W, Winardi S, Kanda H, Goto M. Hydrothermal synthesis: low-temperature subcritical water for ceria-zirconia mixed oxides preparation. Indones J Chem 2021;21:1–13.
[33] Huang PX, Wu F, Zhu BL, Gao XP, Zhu HY, Yan TY, Huang WP, Wu SH, Song DY. CeO2 nanorods and gold nanocrystals supported on CeO2 nanorods as catalyst. J Phys Chem B 2005;109:19169–74.
[34] Campos PTA, Lima JPV, Silva DRD, Oliveira CF, Dias SCL, Dias JA. Cerium-zirconium mixed oxide nanostructures for diesel soot oxidation: synthesis and effect of structure. RSC Adv 2020;10:27428–38.
[35] Zhang XH, Wang Q, Zhang J, Wang JA, Guo MW, Chen SW, Li CH, Hu CW, Xie YC. One step hydrothermal synthesis of CeO2-ZrO2 nanocomposites and investigation of the morphological evolution. RSC Adv 2015;5:89976–84.
[36] Kim JR, Lee KY, Suh MJ, Ihm SK. Ceria-zirconia mixed oxide prepared by continuous hydrothermal synthesis in supercritical water as catalyst support. Catal Today 2012;185:25–34.
[37] Álvarez Moreno A, Ramirez-Reina T, Ivanova S, Roger A-C, Centeno MÁ, Odriozola JA. Bimetallic Ni–Ru and Ni–Re catalysts for dry reforming of methane. Understanding the Synergies of the Selected Promoters 2021;9.
[38] Lyu YM, Jocz J, Xu R, Stavitski E, Sievers C. Nickel speciation and methane dry reforming performance of Ni/CexZr1-xO2 prepared by different synthesis methods. ACS Catal 2020;10:11235–52.
[39] Li JH, Liu ZQ, Cullen DA, Hu WH, Huang JE, Yao LB, Peng ZM, Liao PL, Wang RG. Distribution and valence state of Ru species on CeO2 supports: support shape effect and its influence on CO oxidation. ACS Catal 2019;9:11088–103.
[40] Mai H-X, Sun L-D, Zhang Y-W, Si R, Feng W, Zhang H-P, Liu H-C, Yan C-H. Shape-selective synthesis and oxygen storage behavior of ceria nanopolyhedra, nanorods, and nanocubes. J Phys Chem B 2005;109:24380–5.
[41] Kun-udom R, Jantarang S, Du Z, Kitiyanan B, Rirksomboon T, Meeyoo V. Morphology dependent? Elucidating the catalyst structures of Ni/Ce0.75Zr0.25O2 in the steam reforming of acetic acid. Green Chemical Engineering 2022;3:44–54.
[42] Aribi K, Soltani Z, Ghelamallah M, Granger P. Structure, morphology and reducibility of ceria-doped zirconia. J Mol Struct 2018;1156:369–76.
[43] Safariamin M, Tidahy LH, Abi-Aad E, Siffert S, Aboukaïs A. Dry reforming of methane in the presence of ruthenium-based catalysts. Compt Rendus Chem 2009;12:748–53.
[44] Stuchinskaya TL, Musawir M, Kozhevnikova EF, Kozhevnikov IV. Liquid-phase oxidation of alcohols by oxygen and nitrous oxide catalysed by Ru–Co oxide. J Catal 2005;231:41–7.
[45] Fornasiero P, Trovarelli A, World S. Catalysis by ceria and related materials. 2nd ed. London: Imperial College Press; 2013.
[46] Homsi D, Aouad S, Gennequin C, Aboukaïs A, Abi-Aad E. A highly reactive and stable Ru/Co6–xMgxAl2 catalyst for hydrogen production via methane steam reforming. Int J Hydrogen Energy 2014;39:10101–7.
[47] Djinović P, Osojnik Črnivec IG, Erjavec B, Pintar A. Influence of active metal loading and oxygen mobility on coke-free dry reforming of Ni–Co bimetallic catalysts. Appl Catal B Environ 2012;125:259–70.
[48] Wang JB, Shih W-H, Huang T-J. Study of Sm2O3-doped CeO2/Al2O3-supported copper catalyst for CO oxidation. Appl Catal Gen 2000;203:191–9.
[49] Liu Z, Zhou R, Zheng X. Comparative study of different methods of preparing CuO-CeO2 catalysts for preferential oxidation of CO in excess hydrogen. J Mol Catal Chem 2007;267:137–42.
[50] Chang H, Bjørgum E, Mihai O, Yang J, Lein HL, Grande T, Raaen S, Zhu Y-A, Holmen A, Chen D. Effects of oxygen mobility in La–Fe-based perovskites on the catalytic activity and selectivity of methane oxidation. ACS Catal 2020;10:3707–19.
[51] Bedrane S, Descorme C, Duprez D. Oxygen storage and oxygen mobility on ceria and ceria-zirconia supported noble metals. In: Guerrero-Ruiz A, Rodríguez-Ramos I, editors. Studies in surface science and catalysis. Elsevier; 2001. p. 125–34.
[52] Liu X, Zhou K, Wang L, Wang B, Li Y. Oxygen vacancy clusters promoting reducibility and activity of ceria nanorods. J Am Chem Soc 2009;131:3140–1.
[53] Rocchini E, Vicario M, Llorca J, de Leitenburg C, Dolcetti G, Trovarelli A. Reduction and oxygen storage behavior of noble metals supported on silica-doped ceria. J Catal 2002;211:407–21.
[54] Li J, Liu X, Zhan W, Guo Y, Guo Y, Lu G. Preparation of high oxygen storage capacity and thermally stable ceria–zirconia solid solution. Catal Sci Technol 2016;6:897–907.
[55] Rossignol S, Gérard F, Duprez D. Effect of the preparation method on the properties of zirconia-ceria materials. J Mater Chem 1999;9:1615–20.
[56] Radlik M, Adamowska-Teyssier M, Krzton A, Koziel K, Krajewski W, Turek W, Da Costa P. Dry reforming of methane over Ni/Ce0.62Zr0.38O2 catalysts: effect of Ni loading on the catalytic activity and on H-2/CO production. Cr Chim 2015;18:1242–9.
[57] Wolfbeisser A, Sophiphun O, Bernardi J, Wittayakun J, Fottinger K, Rupprechter G. Methane dry reforming over ceria-zirconia supported Ni catalysts. Catal Today 2016;277:234–45.
[58] Soria MA, Mateos-Pedrero C, Guerrero-Ruiz A, Rodriguez-Ramos I. Thermodynamic and experimental study of combined dry and steam reforming of methane on Ru/ZrO2-La2O3 catalyst at low temperature. Int J Hydrogen Energy 2011;36:15212–20.
[59] Chein RY, Chen YC, Yu CT, Chung JN. Thermodynamic analysis of dry reforming of CH4 with CO2 at high pressures. J Nat Gas Sci Eng 2015;26:617–29.
[60] Mao Y, Zhang L, Zheng X, Liu W, Cao Z, Peng H. Coke-resistance over Rh–Ni bimetallic catalyst for low temperature dry reforming of methane. Int J Hydrogen Energy 2023;48:13890–901.
[61] Cao P, Adegbite S, Wu T. Thermodynamic equilibrium analysis of CO2 reforming of methane: elimination of carbon deposition and adjustment of H2/CO ratio. Energy Proc 2017;105:1864–9.
[62] Rostrupnielsen JR, Hansen JHB. CO2-Reforming of methane over transition metals. J Catal 1993;144:38–49.
[63] Abasaeed AE, Al-Fatesh AS, Naeem MA, Ibrahim AA, Fakeeha AH. Catalytic performance of CeO2 and ZrO2 supported Co catalysts for hydrogen production via dry reforming of methane. Int J Hydrogen Energy 2015;40:6818–26.
[64] Zuber M, Patriarca M, Ackermann S, Furler P, Conceicao R, Gonzalez-Aguilar J, Romero M, Steinfeld A. Methane dry reforming via a ceria-based redox cycle in a concentrating solar tower. Sustain Energy Fuels 2023;7:1804–17.

[65] Cao ANT, Pham CQ, Nguyen TM, Van Tran T, Phuong PTT, Vo DVN. Dysprosium promotion on Co/Al2O3 catalysts towards enhanced hydrogen generation from methane dry reforming. Fuel 2022:324.
[66] Al-Doghachi FAJ, Rashid U, Zainal Z, Saiman MI, Taufiq Yap YH. Influence of Ce2O3 and CeO2 promoters on Pd/MgO catalysts in the dry-reforming of methane. RSC Adv 2015;5:81739–52.
[67] Jagodka P, Matus K, Sobota M, Lamacz A. Dry reforming of methane over carbon fibre-supported CeZrO2, Ni-CeZrO2, Pt-CeZrO2 and Pt-Ni-CeZrO2 catalysts. Catalysts 2021;11.
[68] Whang HS, Choi MS, Lim J, Kim C, Heo I, Chang T-S, Lee H. Enhanced activity and durability of Ru catalyst dispersed on zirconia for dry reforming of methane. Catal Today 2017;293–294:122–8.
[69] Kamiuchi N, Haneda M, Ozawa M. Enhancement of OSC property of Zr rich ceria–zirconia by loading a small amount of platinum. Catal Today 2014;232:179–84.